

A Simple Centricity-based Region Growing Algorithm for the Extraction of Airways

Rafael Wiemker, Thomas Bülow, Cristian Lorenz

Philips Research Lab Hamburg,
Röntgenstrasse 24, 22335 Hamburg
{Rafael.Wiemker, Thomas.Buelow, Cristian.Lorenz}@philips.com

Abstract. The presented algorithm was used to participate in the EXACT09 airway segmentation challenge of the Second International Workshop on Pulmonary Image Analysis (MICCAI 2009). The motivation of the presented simple algorithm mainly is to provide a benchmark what results can be achieved with very basic means in comparison to highly sophisticated algorithms. The presented algorithm uses an entirely local centricity property and an amorphous voxel-based region growing. Furthermore, it uses only raw image density value, no derivatives, or pre-processing filters. The algorithm produces quite reasonable results while being characterized by a very simple implementation, primitive data structures and quick runtime.

Keywords: EXACT09, airway extraction, bronchial tree analysis.

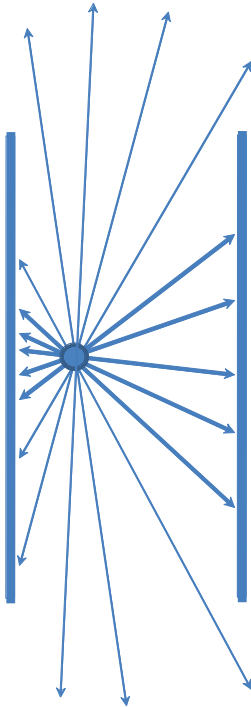
1 Motivation

The motivation of the presented simple algorithm mainly is to provide a benchmark what results can be achieved with very basic means in comparison to highly sophisticated algorithms [1-7] (using e.g. anatomical knowledge, multi-scale, multi-resolution, multi-stage, multi-rule approaches). The presented algorithm is a kind of zero-order algorithm in that it uses an entirely local centricity property and an amorphous voxel-based region growing which is not aware of segments, centerlines, branching points, directional orientation, and does not use tree-specific assumptions such as branching angles etc. It uses only raw image density value, no derivatives, or pre-processing filters.

Earlier papers with participation of the authors of this paper have been based on a front-propagation algorithm [8-14] which was use front-splitting-detection and segment branching heritage. The algorithm discussed here is not related to these earlier works.

2 Algorithmic Details

The algorithm consists only of a voxel-wise centricity measure which is used for a prioritized region growing in conjunction with two termination criteria. The centricity measure aims at quantifying how central a given voxel location is to the surrounding airway.



2.1 Local centricity measure

From a voxel position \mathbf{x} , a number of N rays is cast in a three-dimensional isotropic fashion into all directions. We used N rays sampled on the surface of a sphere according to a recursively subdivided icosahedron. The N rays are pairwise antiparallel in $N/2$ directions. The image density values are sampled in steps of dr along these rays using trilinear interpolation. Each ray is terminated if the density difference to the starting point \mathbf{x} is higher than ΔW (assuming that this means that the airway wall has been encountered), or if becomes longer than a maximum ray length r_{max} . From each two antiparallel radii r_i and r_i' the diameter d_i is computed as $d_i = r_i + r_i'$. Out of the $N/2$ diameters d_i the $N/4$ shortest diameters are selected, i.e. all diameters below the median diameter (assuming that these diameters are approximately normal to the direction of the airway cylinder). From these selected radii the mean R and relative standard deviation σ_R / R is computed. The standard deviation of the radii becomes small or ideally vanishes if \mathbf{x} is located centrally in the surrounding airway. Therefore we define the centricity as $c(\mathbf{x}) = 1 - \sigma_R / R$ (ideally 1 if \mathbf{x} is centered in a surrounding sphere; approximating 1 for a cylinder using the median diameter selection; decreasing to < 0 for strong deviations from a cylinder).

2.2 Prioritized region growing

Starting from a seed point in the trachea (section 2.4), a three-dimensional region growing proceeds (using a 6-neighborhood) into all connected voxels below a certain density threshold D_{air} and above a certain minimum centricity value of $c(\mathbf{x}) \geq c_{min}$. The growth is prioritized by addressing the highest centricity values first.

The growth is otherwise limited only by the following rule: If the mean diameter $R(\mathbf{x})$ for a certain voxel is larger than 2 times the smallest radius encountered on the individual growth path of this voxel (along the path of predecessor voxels), then this voxel is not allowed to spawn any successor voxels.

Due to the centricity prioritization, the growth typically follows along the centerlines. As an optional post-processing step, a local dilation of the grown voxels is performed using the mean radius estimate $R(\mathbf{x})$ around each voxel.

2.3 Runtime and dual-scale-region growing

The median run-time of the algorithm on the training and test datasets was 19 seconds with a rather large standard deviation of 15 sec (on a 3 GHz single processor, using a naïve implementation of ray-casting and tri-linear interpolation). However, in a voxelwise region growing implementation (6-neighborhood) most of the runtime is actually spent to fill the relatively large volume of the trachea. Due to its simple non-delicate structure, the filling of the trachea could be done much more efficiently by other algorithms. On the other hand the paradigm of this algorithm was to keep it as simplistic as possible and not to use hybrid approaches. In a slight deviation from the simplicity-paradigm, we have modified the region-growing such that if the local radius estimation at a certain position is larger than 5 mm, then instead of a single voxel a $3 \times 3 \times 3$ compound-voxel is grown without re-evaluation of the local centricity for each of the additionally included 26 voxels. In this way the average runtime is reduced to 5 sec without changing the results in the finer airways.

2.4 Trachea seed finding

The axial slice images are converted to binary images using a threshold of D_{air} and a two-dimensional connected component analysis is used on each slice to identify blobs with extents below $2 r_{max}$. For each 2D-blob, a figure of merit is computed from its roundness and proximity to the image center. Then an iterative clustering scheme is applied which clusters blobs from adjacent slices to linear structures. These clusters are compared by virtue of mean blob-merit, blob-radius similarity, linear fit goodness, and closeness to craniocaudal orientation, and the best cluster is selected to represent a piece of the trachea, from which a central seed point is derived.

2.5 Parameters

The parameter values were not optimized on the EXACT training datasets, but adopted as sensible values from earlier datasets.

- maxAirwayDensity $D_{air} = -750$ HU
- maxRadiusIncrease = 2
- minimum centricity $c_{min} = 0.0$
- wall density difference $\Delta W = 200$ HU
- number of rays $N = 42$ (antiparallel in 21 different directions)
- sampling step along rays $dr =$ half of smallest voxel size dimension
- maximum ray length $r_{max} = 20$ mm (assuming that even the trachea is less than 40 mm of diameter)

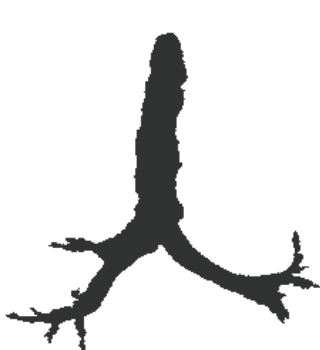
3 Results

An iconing overview over training as well as testing datasets is shown below, as well as an example of worst and best case. Numerical results for all test cases computed by the EXACT09 organizers (P. Lo, M. de Bruijne, B. van Ginneken, J. Reinhardt) are given in Table 1.

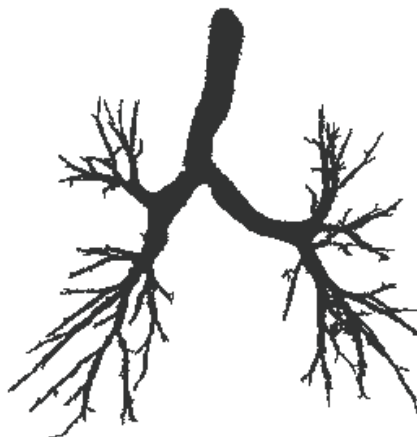
“Training Data”



“Testing Data”



Example CASE38
“worst case”



Example CASE40
“best case”

Table 1: Evaluation measures for the twenty cases in the test set.

	Branch count	Branch detected (%)	Tree length (cm)	Tree length detected (%)	Leakage count	Leakage volumc (mm ³)	False positive rate (%)
CASE21	118	59.3	64.7	58.5	0	0.0	0.00
CASE22	302	78.0	226.8	68.6	84	3726.2	12.12
CASE23	203	71.5	129.9	49.9	62	1184.9	5.13
CASE24	102	54.8	80.8	49.7	0	0.0	0.00
CASE25	116	49.6	86.4	34.3	0	0.0	0.00
CASE26	45	56.3	32.0	48.8	0	0.0	0.00
CASE27	41	40.6	31.2	38.6	0	0.0	0.00
CASE28	82	66.7	56.8	51.8	0	0.0	0.00
CASE29	124	67.4	79.7	57.7	7	155.7	1.58
CASE30	94	48.2	66.0	43.2	0	0.0	0.00
CASE31	128	59.8	85.5	48.7	13	742.8	4.66
CASE32	102	43.8	71.9	33.0	3	199.6	1.12
CASE33	126	75.0	95.6	65.0	7	57.1	0.69
CASE34	953	55.2	165.8	46.4	44	444.1	1.37
CASE35	143	41.6	89.4	28.9	12	82.1	0.46
CASE36	190	52.2	183.2	44.4	2	4.8	0.03
CASE37	104	56.2	71.2	40.1	2	20.5	0.15
CASE38	39	39.8	28.9	43.5	0	0.0	0.00
CASE39	237	45.6	183.7	44.9	27	690.7	3.78
CASE40	231	59.4	181.6	46.9	7	70.5	0.47
Mean	139.0	56.0	100.6	47.1	13.5	368.9	1.58
Std. dev.	73.8	11.4	57.8	10.1	23.4	854.4	2.96
Min	39	39.8	28.9	28.9	0	0.0	0.00
1st quartile	94	45.6	64.7	40.1	0	0.0	0.00
Median	121	55.7	83.1	46.6	3	38.8	0.30
3rd quartile	231	67.4	181.6	57.7	27	690.7	3.78
Max	302	78.0	226.8	68.6	84	3726.2	12.12

4 Discussion

Visual appraisal of the segmentations resulting from the algorithm clearly show a number of airway segments which can be discerned by the human eye but are not segmented by the simple algorithm. Main reasons are image noise, lack of spatial resolution (voxel sampling, slice thickness), and non-connected airway segments (caused by e.g. bronchiolitis, mucus, disease-caused alterations, anomalies, etc.).

Nevertheless, the results of the algorithm can serve as an interesting baseline for the improvements which can be achieved with more sophisticated approaches, which however, usually require many more anatomical models, rules, parameters (with its overfitting pitfalls), run-time and program code (with its maintenance costs). The charm of the algorithm stems from its simple implementation, primitive data structures and quick runtime.

References

1. S.A. Wood, E.A. Zerhouni, J.D. Hoford, E.A. Hoffman, W. Mitzner, Measurement of Three-Dimensional Lung Tree Structures by Using Computed Tomography, *Journal of Applied Physiology*, 79 (5), pp.1687-1697, 1995.
2. A.P. Kiraly, W. Higgins, E. Hoffman, G. McLennan, J. Reinhardt, Three-Dimensional Human Airway Segmentation Methods for Virtual Bronchoscopy, *Academic Radiology*, 9 (10), pp.1153-1168, 2002.
3. J.N. Kaftan, A.P. Kiraly, D.P. Naidich, C.L. Novak, A Novel Multi-Purpose Tree and Path Matching Algorithm with Application to Airway Trees, *SPIE 2006 Medical Imaging Conference*, SPIE vol. 6143, 2006.
4. D. Aykac, E.A. Hoffman, G.McLennan, J.M. Reinhardt, Segmentation and Analysis of the Human Airway Tree From Three-Dimensional X-ray CT Images, *IEEE Trans. Medical Imaging*, 22 (8), pp.940-950, 2003.
5. C. Fetita, F. Preteux, C. Beigelman-Aubry, P. Grenier, Pulmonary airways: 3D reconstruction from multi-slice CT and clinical investigation, *IEEE Trans. on Medical Imaging*, Vol. 23 (11), November 2004, pp. 1353-1364.
6. J. Tschirren, E.A. Hoffman, G. McLennan, M. Sonka, Segmentation and Quantitative Analysis of Intrathoracic Airway Trees from Computed Tomography Images, *Proc. American Thoracic Society 2*, pp.484-487, 2005.
7. J. Tschirren, E.A. Hoffman, G. McLennan, M. Sonka, Intrathoracic Airway Trees: Segmentation and Airway Morphology Analysis From Low-Dose CT Scans, *IEEE Transactions on Medical Imaging*, Vol. 24 (12), December 2005, pp.1529-1539.
8. Schlathölter, T., Lorenz, C., Carlsen, I.C., Renisch, S., Deschamps, T., Simultaneous segmentation and tree reconstruction of the airways for virtual bronchoscopy, *Proc. SPIE 2002*, vol.4684, pp.103-113.
9. R. Wiemker, T. Blaffert, T. Bülow, S. Renisch, C. Lorenz, Automated assessment of bronchial lumen, wall thickness and bronchoarterial diameter ratio of the tracheobronchial tree using high-resolution CT, *Proc. Computer Assisted Radiology and Surgery*, CARS 2004, pp. 967-972.
10. R. Wiemker, A. Ekin, R. Opfer, T. Bülow, P. Rogalla, Unsupervised Extraction and Quantification of the Bronchial Tree on Ultra-Low-Dose vs. Standard Dose CT, *SPIE 2006 Medical Imaging*, SPIE vol. 6143, 2006.
11. T. Bülow, C. Lorenz, S. Renisch: A General Framework for Tree Segmentation and Reconstruction from Medical Volume Data. *MICCAI 2004*, p.533-540.
12. T. Bülow, C. Lorenz, R. Wiemker, J. Honko, Point based methods for automatic bronchial tree matching and labeling, *Proc. SPIE 2006 Medical Imaging Conference*, San Diego, SPIE vol. 6143, 2006.
13. T. Bülow, R. Wiemker, T. Blaffert, C. Lorenz, S. Renisch, Automatic Extraction of the Pulmonary Artery Tree from Multi-Slice CT Data, *Proc. SPIE 2005 Medical Imaging Conference*, SPIE vol. 5746, pp.730-740, 2005.
14. Wiemker, R., Bülow T., Opfer R., Automated Hierarchical Partitioning of Anatomical Trees, *Proc. SPIE 2007 Medical Imaging Conference*, SPIE vol. 6511.